

# Contrasting Effects of Dissimilatory Iron(III) and Arsenic(V) Reduction on Arsenic Retention and Transport

BENJAMIN D. KOCAR,<sup>†</sup>  
MITCHELL J. HERBEL,<sup>‡</sup>  
KATHERINE J. TUFANO,<sup>†</sup> AND  
SCOTT FENDORF\*,<sup>†</sup>

Department of Geological and Environmental Sciences,  
Stanford University, Stanford, California 94305, and  
USDA-ARS-USSL, George E. Brown, Jr., Salinity Laboratory,  
450 West Big Springs Road, Riverside, California 92507

Reduction of arsenate As(V) and As-bearing Fe (hydr)-oxides have been proposed as dominant pathways of As release within soils and aquifers. Here we examine As elution from columns loaded with ferrihydrite-coated sand presorbed with As(V) or As(III) at circumneutral pH upon Fe and/or As reduction; biotic stimulated reduction is then compared to abiotic elution. Columns were inoculated with *Shewanella putrefaciens* strain CN-32 or *Sulfurospirillum barnesii* strain SES-3, organisms capable of As(V) and Fe(III) reduction, or *Bacillus benzoovorans* strain HT-1, an organism capable of As(V) but not Fe(III) reduction. On the basis of equal surface coverages, As(III) elution from abiotic columns exceeded As(V) elution by a factor of 2; thus, As(III) is more readily released from ferrihydrite under the imposed reaction conditions. Biologically mediated As-reduction induced by *B. benzoovorans* enhances the release of total As relative to As(V) under abiotic conditions. However, under Fe reducing conditions invoked by either *S. barnesii* or *S. putrefaciens*, approximately three times more As (V or III) was retained within column solids relative to the abiotic experiments, despite appreciable decreases in surface area due to biotransformation of solid phases. Enhanced As sequestration upon ferrihydrite reduction is consistent with adsorption or incorporation of As into biotransformed solids. Our observations indicate that As retention and release from Fe (hydr)oxide(s) is controlled by complex pathways of Fe biotransformation and that reductive dissolution of As-bearing ferrihydrite can promote As sequestration rather than desorption under conditions examined here.

## Introduction

Arsenic is a toxic metalloid widely distributed in the earth's crust that is adversely impacting human health globally, most notably in Southeast Asia. Prolonged exposure may lead to chronic arsenic toxicosis, a condition encapsulating a variety of diseases including skin lesions and various cancers. In Bangladesh alone, over 57 million people as of 2003 were exposed through regular ingestion of drinking water containing As concentrations in excess of WHO and U.S. drinking water standards of 10  $\mu\text{g L}^{-1}$  (1).

The common valence states of As found in natural waters, As(V) and As(III), exist as arsenate (As(V), as  $\text{H}_2\text{AsO}_4^{x-3}$ ) and arsenite (As(III), typically as  $\text{H}_3\text{AsO}_3$ ). Arsenic mobility is generally considered to be mediated by ligand exchange and reduction–oxidation (redox) reactions (2). Release (desorption) of As during the onset of reducing conditions and ensuing reductive dissolution of As-bearing Fe (hydr)oxides is generally ascribed as the dominant means of displacement from the solid phase (3–5). This hypothesis is often supported by correlations between As and oxalate (solid phase) extractable Fe(III) in contaminated aquifer sediments as well as correlations between Fe(II) and soluble As in well waters (3, 4).

Iron (hydr)oxides retain both As(V) and As(III) (8) and thus often control the dissolved concentration of this element in soils (2). Specific soil/sediment conditions, such as pH and competing adsorbates (6, 7), along with solid properties, such as surface area, may govern the As binding capacities of iron (hydr)oxides. Thus, dissolution and transformation of the iron (hydr)oxides will impart a pronounced effect on As partitioning. Ferrihydrite, a short-range order material common in soils and sediments, is transformed to lower surface area minerals such as goethite and magnetite in the presence of aqueous Fe(II) (8, 9). Thus, iron reduction should be expected to induce As release (desorption) from sediments as Fe(III) (hydr)oxides dissolve or are transformed to lower surface area minerals.

The relative binding affinity of As(III) and As(V) for soil and sediment solids may vary, and thus transformations between these species may also govern the mobility of As. Arsenic(III) binds to Fe(III) (hydr)oxides more extensively than As(V) under circumneutral conditions (6), but As(III) was contrarily shown to be more mobile under flow conditions than As(V) (10). Although As redox transformations may be influenced by abiotic reactions, microorganisms appear to commonly dominate the redox chemistry of As and are capable of reducing As(V) in solution or adsorbed on the surfaces of Fe and Al (hydr)oxides (11). Indeed, many organisms have been isolated that transform As either through respiratory and/or detoxification pathways (12, 13). Isolated organisms include *Sulfospirillum barnesii* strain SES-3, a Gram negative vibrio capable of respiring on Fe(III) and As(V) (14), and *Shewanella putrefaciens* strain CN-32, a Gram negative rod also capable of Fe(III) respiration (15) and recently identified as capable of respiring on As(V) (16). Although these organisms are capable of both Fe(III) and As(V) reduction, other organisms, such as the Gram positive rod *Bacillus benzoovorans* strain HT-1, lack the ability to reduce Fe(III) but reduce (and likely respire on) As(V) (17).

The growing number of isolated bacteria with known metabolisms makes it possible to manipulate biologically induced chemical conditions within model systems in order to deduce principal mechanisms responsible for As release from the solid phase. Therefore, the objectives of our study were to (1) examine the desorption of As from ferrihydrite-coated quartz sand under As and/or Fe reducing conditions and (2) identify the specific processes controlling As release (or retention). Here we observe that As is retained within column solids under Fe reducing conditions and that within our system As reduction mobilizes As to a greater degree than the dissolution of ferrihydrite.

## Materials and Methods

**Column Experiments.** Arsenic elution was observed from a suite of columns containing As presorbed to ferrihydrite coated quartz sand. Ferrihydrite was synthesized (18),

\* Corresponding author phone: (650)723-5238; e-mail: fendorf@stanford.edu.

<sup>†</sup> Stanford University.

<sup>‡</sup> USDA-ARS-USSL.

centrifuged, and rinsed with doubly deionized (DDI) water. Ferrihydrite was then mixed with quartz sand (8), dried, and resuspended into an artificial groundwater solution (pH 7.2) containing 2.7 mM KCl, 0.6 mM MgSO<sub>4</sub>, 7.9 mM NaCl, 0.2 μM NH<sub>4</sub>Cl, 0.4 mM CaCl<sub>2</sub>, 3.7 mM NaHCO<sub>3</sub>, 0.1 mL L<sup>-1</sup> Wolfe's Minerals, 1 mM sodium lactate, and 10 mM PIPES buffer. The final loading of ferrihydrite on quartz sand was approximately 10 g kg<sup>-1</sup>. Phosphate was presorbed to the ferrihydrite coated quartz sand at a loading of 1 mg kg<sup>-1</sup> to facilitate microbial growth. After equilibration for 3 d, the phosphate solution was decanted and soluble As(III) or As(V) was added to achieve the desired As surface coverage based on adsorption isotherms (19). For columns containing As(V), coverages of 10, 30, and 50% of the adsorption maximum were used, corresponding to solid concentrations of approximately 80, 200, and 400 mg kg<sup>-1</sup> (As on ferrihydrite coated quartz sand). For columns using As(III), a 50% coverage was used, corresponding to 800 mg kg<sup>-1</sup>. After a 3 d reaction period, the As-bearing solution was decanted, and the As-ferrihydrite-quartz slurry was rinsed several times with fresh simulated groundwater.

*Shewanella putrefaciens* (CN-32), *Sulfurospirillum barnesii* (SES-3), and *Bacillus benzoovorans* (HT-1) were grown to late-exponential phase. *S. putrefaciens* was grown for 12 h under aerobic conditions in tryptic soy broth at 25 °C; *S. barnesii* and *B. benzoovorans* were cultured for 3 d in the media SeFr1 under anaerobic conditions (19). All microbial species were centrifuged and resuspended in groundwater several times before addition to the As-mineral slurry. They were then mixed under anaerobic conditions into the As-mineral slurry to achieve an initial cell loading of ~10<sup>8</sup>–10<sup>9</sup> cells g<sup>-1</sup>. The slurry was then loaded into 25 cm long columns with a radius of 3.8 cm. Artificial groundwater solution was delivered to the column(s) at a rate of 1 pore volume d<sup>-1</sup>.

After being passed through a 0.22 μm filter, effluent concentrations of Fe and As were measured as a function of time using inductively coupled plasma atomic emission spectrometry (ICP-AES), with a detection limit of 2.67 μM. Samples with low (<7 μM) As were also analyzed using hydride generation (HG-ICP-AES), which achieved a detection limit of 93 nM As. Lactate and acetate were analyzed by ion chromatography (As6 column, Dionex Corp.), and selected samples were analyzed for As(V) and As(III) using ion chromatographic separation with HG-ICP-AES detection (20).

Columns were typically eluted for 25 to 30 d; upon the termination of flow, solid phases were harvested at regular spatial intervals. All column experiments as well as initial column preparation procedures were carried out in an anaerobic glovebag (95% N<sub>2</sub>, 5% H<sub>2</sub>). Reacted solid phases were dried and analyzed for surface area, total As, Fe(II), and total Fe; a subset of the solid (untreated) was saved for subsequent X-ray absorption spectroscopic (XAS) analysis. Iron(II) concentrations from 6 M HCl digests were measured using the ferrozine method (21).

Cell counts were performed both at the beginning and end of experimentation by resuspending solids in pyrophosphate, mixing, and fixing with glutaraldehyde. Cells were stained with 4',6-diamidino-2-phenylindole (DAPI) and counted using epifluorescence microscopy.

#### Batch Desorption of As from Ferrihydrite Coated Sand.

Experiments were conducted to determine the effect of dissolved aqueous constituents and cellular components on As desorption from ferrihydrite coated sands under batch conditions. Approximately 2 g of As(III) or As(V) sorbed (20% surface coverage) on ferrihydrite coated sands were added to 50 mL of artificial groundwater. Lactate, NaHCO<sub>3</sub>, and FeCl<sub>2</sub> (all 1 mM) were added to elucidate their effects on As desorption. Separate batch experiments containing γ-irradiated (2 Mrad, 10<sup>9</sup> cells g<sup>-1</sup>) cells of *S. barnesii* and 2 g

of As(III) or As(V) sorbed ferrihydrite coated sand were performed to examine the effect of cellular components on As release from the coated sands. All samples were placed on an orbital shaker at 100 rpm; at 18 h, 2.0 mL of solution were removed from the bottles, filtered (0.2 μm), and acidified with 0.1 M HCl for As and Fe analysis.

**Solid-Phase Analysis.** Arsenic local structure for a subset of column samples was determined using XAS analysis at the Advanced Photon Source. Extended X-ray absorption fine structure (EXAFS) spectra were obtained on beamline 13-BM using an unfocused beam and a Si(111) crystal monochromator. X-ray fluorescence was measured using a 13 element Ge detector. Spectra were collected from -150 to 867 eV relative to the As K edge of 11 867 eV; energy calibration was achieved via scanning dilute Na<sub>3</sub>AsO<sub>4</sub> after every third sample and setting the first derivative inflection point to 11 874 eV. Iron EXAFS spectra were collected at beamline 11-2 at the Stanford Synchrotron Radiation Laboratory. A double crystal Si(220) monochromator was used for energy selection. Scans were conducted from 100 eV below to 1000 eV above the Fe K-edge at 7111 eV.

Both As and Fe fluorescence spectra were averaged and normalized to unity using the XAS data reduction software SIXPACK (22). SIXPACK/IFEFFIT algorithms were used to isolate backscattering contributions by subtracting a spline function from the EXAFS data region. The resulting function was then converted from units of eV to Å<sup>-1</sup>, weighted by k<sup>3</sup>, and windowed from 3 to 14 Å<sup>-1</sup>. Linear combination of model compounds was performed to reconstruct unknown spectra; no more than four standards were varied at a time, and Fe(II)-phases were constrained to obtain mass balance (within 5%) with extractable Fe(II). Model compound (standards) contributions were deemed significant if their mole percentage was greater than 10%, albeit that we could reproduce magnetite in mixed standards to a level of 5%. Ferrihydrite, magnetite, and goethite were first fit to unknown spectra with arbitrary initial values. Other model compounds for linear combination Fe EXAFS fitting included ferrihydrite sorbed to quartz sand, green rust-chloride, green-rust sulfate, green-rust carbonate, hematite, lepidocrocite, synthetic and natural siderite, vivianite, and amorphous FeS. Model compounds used in As EXAFS linear combination fitting included Na<sub>3</sub>AsO<sub>4</sub>, NaAsO<sub>2</sub>, HAsO<sub>4</sub><sup>2-</sup>(aq), As(OH)<sub>3</sub>(aq), As(III) sorbed to ferrihydrite, As(V) sorbed to ferrihydrite, scorodite, orpiment, realgar, and arsenopyrite. Arsenic linear combination fitting was identical to that used with Fe. Model spectra of As(III) and As(V) (50% coverage) sorbed to ferrihydrite were used as initial components during fitting, and other components were tested thereafter.

To quantify Fe(II)-As(III) precipitates potentially occurring within column experiments, a fresh Fe(II)-As(III) precipitate was examined with Fe and As XAS. The solid was prepared by slowly (over several minutes) adding 1 mM Fe(II) to 1 mM As(III) at 25 °C, buffered at pH 7.2 with either PIPES or bicarbonate. The resulting solid phase was then deposited on a filter, rinsed with DI water, dried, and sealed in Kapton tape. Iron and As XAS analysis were performed on the solid phase as described above and used as a model compound in Fe linear combination fitting. Both Fe and As local structure (not shown) were similar to that recently described by Thorar et al. (23).

## Results

**Arsenic Release from Ferrihydrite Coated Sands.** Arsenic eluted at variable rates from columns, depending on As speciation and the presence of bacteria capable of respiring on Fe and/or As. Upon initiation of artificial groundwater flow, greater quantities of As(III), rather than As(V), elute from abiotic columns possessing a 50% initial surface coverage (Figure 1, Table 1). In fact, more than four times

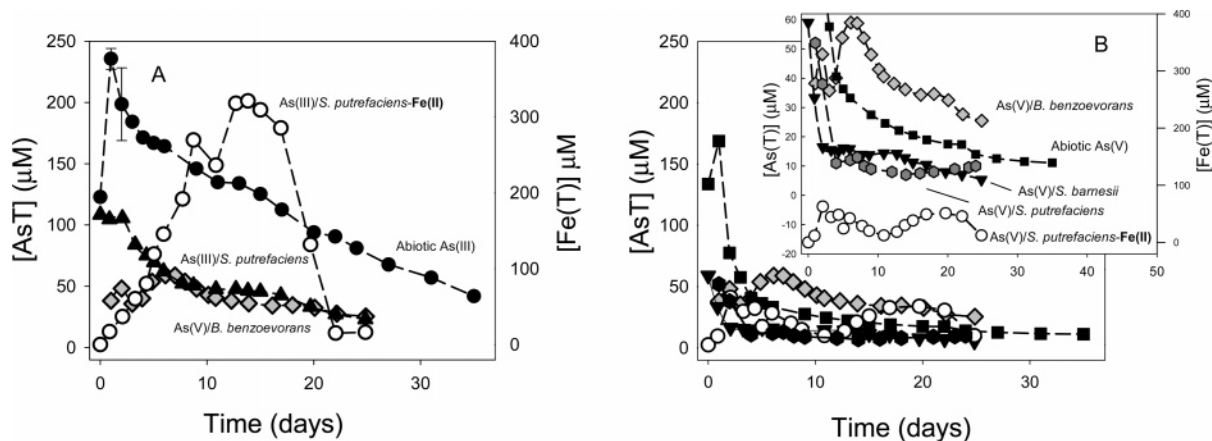


**FIGURE 1.** (A) Arsenic elution from abiotic and biotic (*S. putrefaciens*) columns initially containing As(III)-ferrihydrite-quartz (closed symbols), soluble Fe elution from the As(III)-*S. putrefaciens* column (open circles). Error bars represent standard error from duplicate measurement of abiotic column samples. (B) Arsenic elution from abiotic and biotic (*S. putrefaciens* and *S. barnesii*) columns initially containing As(V)-ferrihydrite-quartz (closed symbols) and iron elution from the As(V)-*S. putrefaciens* column (open circles). Arsenic elution from a biotic column containing *B. benzoovorans* (HT-1) initially containing As(V)-ferrihydrite-quartz is plotted on both graphs for comparison. Experimental conditions for all columns: 50% As surface coverage (with the exception of the *S. barnesii* column, 30% As(V) coverage) and flow rate of 1 pore vol. d<sup>-1</sup> of artificial groundwater.

**TABLE 1. Bacterial Characteristics, Solid-Phase Chemistry and Sorbed Species, and Elution of As from Column Experiments.**

bacteria used in column expts	e- acceptor		initial Fe loading, mg kg <sup>-1</sup> (mmol column <sup>-1</sup> )	initial As loading, μmol kg <sup>-1</sup> (μmol column <sup>-1</sup> )	surface coverage <sup>a</sup> (%)	As eluted at 25 d (μmol)	percent initial As eluted (25 d)	initial cell counts (cells/g)	final cell counts (cells/g)
	As(V)	Fe(III)							
abiotic			6885 (24.7)	5500 (1237)	50 As(V)	131	11		
abiotic			9505 (34.0)	10117 (2276)	50 As(III)	508	22		
<i>S. putrefaciens</i>	+	+	4895 (17.5)	5779 (1300)	50 As(V)	47	4	2.5E8	2.3E7
<i>S. putrefaciens</i>	+	+	5942 (21.3)	11866 (2670)	50 As(III)	196	7	1.7E9	5.9E8
<i>S. barnesii</i>	+	+	3973 (14.2)	2682 (604)	30 As(V)	45	7	1.7E9	1.0E8
<i>S. barnesii</i>	+	+	5290 (18.9)	1081 (243)	10 As(V)	0.002	<0.001	1.1E9	7.5E7
<i>B. benzoovorans</i>	+	-	3565 (12.7)	6433 (1448)	50 As(V)	114	8	3.9E8	5.3E7

<sup>a</sup> Surface coverage determined using the Langmuir isotherm adsorption maxima (19).

the cumulative amount of As(III) (508 μmol) elute as compared to As(V) (131 μmol). Owing to the variation in initial surface coverage, 22% of the total As(III) is released as compared to 11% for As(V) (Table 1).

Surprisingly, under Fe reducing conditions invoked by *S. putrefaciens*, over three times more As is retained, not released, within a column initially loaded with As(III) as compared to an abiotic (control) column (Figure 1, Table 1). After 1 d, As effluent concentrations from the As(III)-*S. putrefaciens* column are less than half of the abiotic control. The decrease in effluent As concentration from the As(III)-*S. putrefaciens* column coincides with the production of Fe(II) (Figure 1). Ferrous iron concentrations exceed 100 μM after 6 d, eventually rising to a peak concentration of 300 μM at 13 d and falling below 50 μM after 22 d (Figure 1A). Although less dramatic, As elution also decreased during combined Fe and As(V) reduction relative to an abiotic column loaded with As(V) (Figure 1B). About three times as much As eluted from the abiotic control (a total of 131 μmol As or 11% of total column As) compared to the As(V)-*S. putrefaciens* column (47 μmol As or 4% of total column As) (Table 1); Fe(II) concentrations within the biotic column peak at approximately 100 μM. Arsenic release from ferrihydrite coated sands with As(V) and *S. barnesii* yield nearly indistinguishable results with *S. putrefaciens* (Figure 1). Additionally, As(III) is the only species detected in the porewater after 2 d and is the dominant species present in the solid phase upon column breakdown (25–30 d). At lower As coverage (10% of adsorption maximum), ferrihydrite is extensively biotransformed (Table 2), and Fe(II) concentrations peaked at nearly 600 μM (Table 1; Figure S3). Although column

effluent concentrations of As were detectable over the first several days, they decreased as a function of time from 300 nM to 60 nM (1 and 4 d, respectively). After this time, As effluent concentrations are below the detection limit. Less than 0.001% of the total column As eluted, indicating As is retained despite (or as a result of) extensive iron transformation.

Relative to the abiotic As(V) column (Figure 1), As desorption increases as a result of As(V) reduction by *B. benzoovorans* (HT-1) (initial coverage of 50% adsorption maximum). Arsenic effluent concentrations initially mimic abiotic elution of As(V) (Figure 1) and then increase as a function of time. This pattern of elution is explained by the reduction of As(V) to As(III) and subsequent As desorption—after 2 d, less than 1% of the effluent As remained in the pentavalent state. Concentrations of As do not reach those of comparable abiotic column since (i) 50% initial coverage of As(V) is approximately half that of a 50% As(III) coverage and (ii) As(III) is progressively generated.

#### Batch Desorption of As from Ferrihydrite-Coated Sands.

In batch experiments, approximately 30–45% of either As(V) or As(III) desorb upon addition of artificial groundwater (control), 1 mM bicarbonate, or 1 mM lactate (Figure 2). Compared to the control (groundwater addition only), lactate and bicarbonate addition do not impact As(V) or As(III) desorption. The addition of 1 mM Fe(II), in contrast, decreases the amount of As(V) desorption (i.e., it increases retention) by a factor of 3. Ferrous-Fe also decreases the desorption of As(III), although to a lesser extent than for As(V) (Figure 2). Simultaneous addition of Fe(II), lactate, and bicarbonate results in desorption similar to the Fe(II) treatment. Darken-



TABLE 2. Column Solid-Phase Characteristics<sup>a,b</sup>

distance from inlet (cm)	Fe(T) <sup>c</sup> (mg kg <sup>-1</sup> )	Fe(II) <sup>c</sup> (mg kg <sup>-1</sup> )	As(T) <sup>c</sup> (mg kg <sup>-1</sup> )	As(III): As(V) <sup>d</sup>	surface area <sup>e</sup> (m <sup>2</sup> g <sup>-1</sup> )	dominant iron mineralogy <sup>f</sup> (mol %)	
						ferrihydrite	magnetite
Abiotic Column with As(III)							
start	9505 (882)		758 (80)	100:0			
15–20	6004 (1902)		381 (118)				
10–15	7040 (894)		375 (49)				
5–10	7353 (31)		281 (10)				
0–5	7010 (914)		146 (50)				
Abiotic Column with As(V)							
start	6885 (971)		412 (105)	0:100			
15–20	6515 (544)		365 (40)				
10–15	7549 (1066)		411 (69)				
5–10	6042 (469)		274 (21)				
0–5	5704 (723)		221 (44)				
Column with CN-32 and As(V)							
start	4895 (95)		433 (20)	0:100	3.18	100	
15–20	4818 (51)	89 (15)	396 (12)	43:57	1.88	91	9
10–15	4793 (59)	86 (11)	405 (11)	35:65	1.65	93	7
5–10	4521 (128)	68 (12)	353 (13)	19:81	1.68	90	10
0–5	4805 (56)	134 (29)	314 (25)	49:51	1.89	91	9
Column with CN-32 and As(III)							
start	5942 (101)		889 (29)	100:0	3.31	100	
15–20	5954 (189)	275 (39)	1047 (51)		2.01	89	11
10–15	6066 (145)	320 (46)	904 (23)		2.25	85	15
5–10	5838 (314)	217 (16)	905 (21)		2.23	89	11
0–5	5979 (94)	219 (22)	596 (13)		2.41	90	10
Column with SES-3 and As(V) (30% As Surface Coverage)							
start	3973		201	0:100			
15–20	2692	827	64	41:59			
10–15	2514	823	161	43:57			
5–10	2340	687	149				
0–5	2756	53	94	26:74			
Column with SES-3 and As(V) (10% As Surface Coverage)							
start	5290 (79)		81 (2)	0:100			
20–24	5345 (88)	1131 (128)	63 (1)	78:22			
16–20	5426 (113)	1259 (38)	66 (10)				
12–16	5460 (84)	1182 (123)	93 (16)	76:24			
8–12	5087 (3)	1165 (66)	74 (16)				
4–8	4496 (186)	1053 (52)	68 (7)	64:36			
0–4	4240 (108)	1091 (10)	58 (6)				
Column with HT-1 and As(V)							
start	3472 (17)		482 (129)	100:0			
16–20	3565 (64)		307 (6)				
12–16	3486 (15)		308 (9)				
8–12	3573 (250)		332 (19)				
4–8	3463 (18)		282 (34)				
0–4	3200 (496)		167 (29)				

<sup>a</sup> Arsenic surface coverages were 50% of maximum (see text) unless otherwise noted. <sup>b</sup> Values in parentheses represent standard error from triplicate digestions. <sup>c</sup> Fe(T), Fe(II), and As(T) values were determined from HCl extraction and ICP/ferrozine analysis. <sup>d</sup> Determined with As EXAFS linear combination fitting. <sup>e</sup> Standard error of BET method was less than  $\pm 0.06 \text{ m}^2 \text{ g}^{-1}$  for all samples. <sup>f</sup> Determined with Fe EXAFS linear combination fitting.

ing of the ferrihydrite illustrates mineralogical changes upon Fe(II) addition, with ~20% of the added Fe(II) being sorbed.

The same series of batch experiments was conducted with killed *S. barnesii* cells to examine the effect of cellular components on As desorption (Figure 2). Once again, Fe(II) addition (by itself or concomitant with lactate and bicarbonate addition) limits (rather than promotes) As(V) and As(III) desorption from the solid phase, whereas lactate addition does not have an appreciable effect on As desorption. Bicarbonate addition in the presence of killed cells appears to enhance As retention. However, a small amount of Fe(II) is generated in this control, likely from residual Fe(III) reductase activity in lysed cells, and may enhance retention similar to 1 mM Fe(II) additions.

**Solid Phase and As Transformations.** Ferrihydrite is partially transformed to magnetite in all columns containing

*S. putrefaciens* (Figure 3, Table 2). Ferrous iron is known to induce the solid-phase transformation of ferrihydrite to magnetite and goethite (8, 9), although goethite is not detected in any of our columns. The least amount of transformation occurs in columns containing As(V), and the most extensive transformation occurs in the column containing As(III), albeit that the differences in transformation, based on ferrihydrite conversion to magnetite, are minimal (Table 2). Paralleling the ripening of ferrihydrite to magnetite is an overall decrease in surface area. The surface area of ferrihydrite coated sand was initially 3.18 (As(V) column) and 3.31 m<sup>2</sup> g<sup>-1</sup> (As(III) column), but it decreases to an average value of 1.78 (As(V) column) and 2.23 m<sup>2</sup> g<sup>-1</sup> (As(III) column) at the end of experimentation (Table 2).

Upon breakdown of biotic experiments, substantial solid phase associated As(III) is detected (Table 2 and Supporting

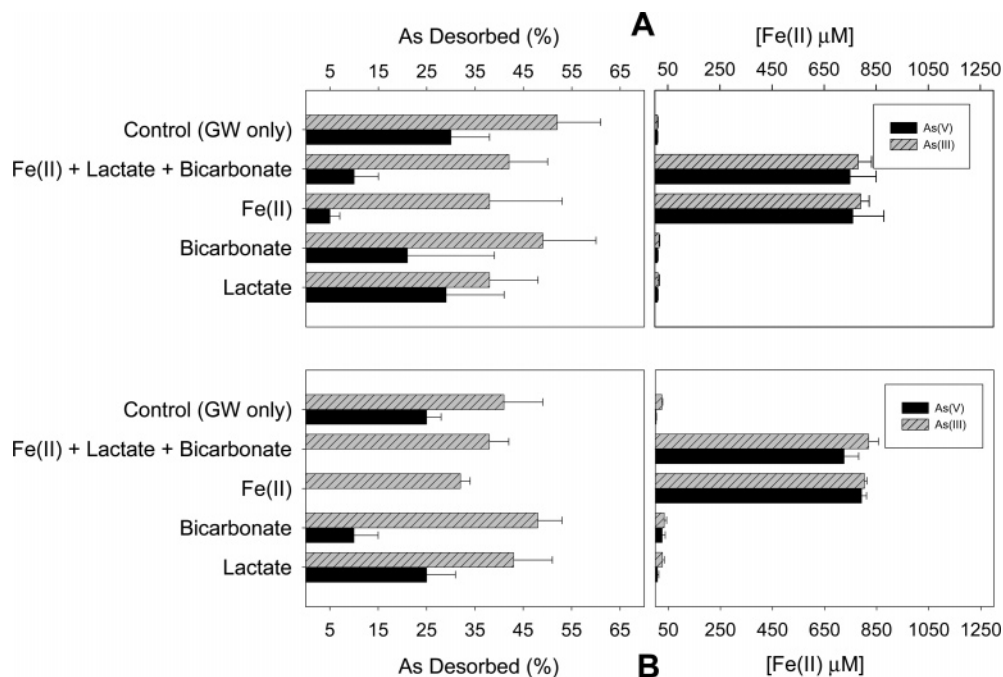


**FIGURE 2.** (A) Arsenic desorption and Fe concentration as a function of artificial groundwater (control), Fe(II), bicarbonate, and lactate addition to batch experiments containing 2 g of As(V)- or As(III)-ferrihydrite-quartz (20% coverage, see text). Concentrations of bicarbonate, lactate, and Fe(II) were 1 mM. (B) Arsenic desorption and Fe concentration in identical batch experiments with the addition of  $\gamma$ -irradiated (killed) *S. barnesii* to all treatments ( $10^9$  cells  $g^{-1}$  As-ferrihydrite-quartz).

Information, Figure S4), even for columns initially loaded with As(V). Within the abiotic columns, As(V) is retained to a greater extent than As(III) (11% elution vs 22% elution, Table 1). Similarly, among biotic columns having 50% As coverage, the greatest extent of As retention occurs within those initially loaded with As(V) (Figure 1B, Table 1), even though much of the As(V) is reduced to As(III) by the end of the experiment (Table 1). Within the As(III) columns, solid-phase extracts and speciation of As within the starting and bioreacted materials confirmed As(III) as the sole species.

## Discussion

Under anaerobic soil or sediment conditions, Fe(III) (hydr)-oxides undergo reductive dissolution, releasing Fe(II) to solution which in turn may induce the transformation of less thermodynamically favorable phases, such as ferrihydrite, to more thermodynamically stable minerals such as goethite and magnetite that often (coincidentally) possess lower surface areas (9, 24). Intuitively, As may be released during these transformations owing to the dissolution (noted by production of Fe(II)) and decrease in surface area of Fe phases. However, this suite of experiments indicates As is retained, relative to abiotic controls, in ferrihydrite columns undergoing iron reduction where both reductive dissolution and an overall decrease in surface area occur.

**Speciation Effects and Retention Mechanisms.** Arsenic(III) elution is greater than that of As(V) in abiotic columns by a factor of 2 based on the proportion of initial As eluted after 25 d (Table 1). About twice as much As(III) sorbs to ferrihydrite coated sand than As(V) at 50% surface coverage. Therefore, As(V) is expected to elute at a greater rate and extent than As(III) if it is assumed that the extent of surface coverage is proportional to binding strength (i.e., binding strength is proportional to the amount of As sorbed at a particular surface coverage; in this case, 50% of the maximum coverage for each species). However, in this case, binding strength (as noted by desorption rate) does not apparently correlate with extent of adsorption. Unfortunately, X-ray techniques used to determine inner-sphere coordination

environments are not always sensitive to potentially labile, outer-sphere complexes, which are possibly more sensitive to perturbations in aqueous concentrations (flow conditions).

The effect of As(V) reduction to As(III) on desorption is pronounced in the column experiment inoculated with *B. benzoovorans* (Figure 1). Elution of As first appears similar to the abiotic column containing As(V), but then eluent As concentration increases as As(V) is reduced and As(III) dominates the dissolved phase (99% of porewater As is As(III) at times greater than 2 d). Although total As elution from the abiotic As(V) column surpassed the As(V)-*B. benzoovorans* column (Table 1), effluent As concentrations at the end of experiment are appreciably greater from the As(V)-*B. benzoovorans* column (Figure 1); thus, As reduction leads to increased desorption and subsequent elution. This experiment also illustrates that cellular matter did not enhance As retention since As desorption increases during microbially driven As(V) reduction compared to the abiotic As(V) column. Similarly, arsenic desorption is not appreciably affected by the addition of killed *S. barnesii* cells (Figure 2) in batch experiments (not containing Fe(II)), relative to controls containing only groundwater and As sorbed to ferrihydrite.

Upon initiation of iron reduction, both As(III) and As(V) are retained relative to abiotic columns (Figure 1). Enhanced As retention occurs during iron reduction irrespective of initial As speciation, although the greatest relative difference (in terms of quantity of As retained during iron reduction compared to As retained in abiotic controls) occurs with concurrent As(V) reduction. The pronounced decrease in As(III) elution (increased As retention) under iron reducing conditions is striking, mainly because As(III) elutes to a much greater extent from the abiotic column. Ferrous iron also increases As(III) retention within batch experiments (which contain ferrihydrite), in contrast to other studies which have implicated Fe(II) in As desorption from (natural) Fe (hydr)-oxides (25). However, As(V) is retained to a greater extent than As(III) in the presence of cellular material and Fe(II) (Figure 2), again illustrating that a retention mechanism involving Fe(II) is not necessarily limited to As(III) production.

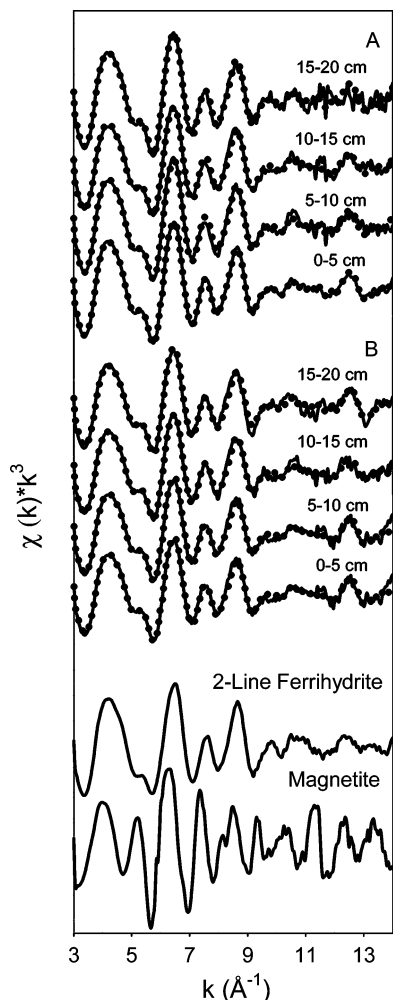


**FIGURE 3.** Least-squares fits (dotted lines) to experimental  $k^3$  weighted Fe-EXAFS spectra (solid lines) obtained for solids (column section lengths given in cm) from columns initially containing (A) As(III)-ferrihydrite-quartz and *S. putrefaciens* and (B) As(V)-ferrihydrite-quartz and *S. putrefaciens*.

Amine groups are thought to play a role in As(V) adsorption to humic acids (26), and cations may enhance adsorption of As(V) to humic acids by acting as bridging compounds (27). Artificial groundwater constituents and Fe(II) may enhance As(V) binding to cellular matter in our experiments. Overall, the plethora of functional groups present in cells appear to be a potential sink of As(V) within bioreacting columns, but, in contrast, As(III) retention is not increased by cellular matter. Thus, enhanced retention of As within columns, dominantly as As(III), cannot be solely explained by adsorption to cells and cellular matter.

**Solid-Phase Precipitation and Transformation Influencing As Solubility.** Although appreciable concentrations of Fe(II) and magnetite formed within our column solids, neither was as extensive as in previous work under similar experimental conditions but without As (8, 9). Both oxyanions of As poison the ripening of ferrihydrite to lepidocrocite or goethite. Additionally, As, as either As(V) or As(III), depresses the Fe(II) concentration (extent of iron reduction) and thereby depresses magnetite formation. High As concentrations may induce a toxic effect upon basal metabolic pathways, such as substrate-level phosphorylation, or inhibit sulfhydryl-bearing enzymes, thus potentially slowing the biogenic production of Fe(II). However, lactate oxidation (see the Supporting Information, Figures S1 and S2) indicates that metabolic activity was sustained upon As addition. Thus, it

is likely that arsenic oxyanions alter the surface chemistry of ferrihydrite sufficiently to decrease dissimilatory Fe(III) reduction.

Enhanced retention of arsenic noted upon reductive transformation of ferrihydrite may result from either the formation of an Fe(II)-As(III) precipitate (23) or via incorporation of As in or on secondary precipitates. We were unable to detect an Fe(II)-As(III) solid phase in the reaction products, however, implicating the latter mechanism. Additionally, arsenic sequestration is not observed in goethite-coated sand columns having comparable Fe(II) concentrations (data not shown), where minimal Fe(III) biotransformation results. Thus, enhanced As(III) retention appears dependent on remineralization of iron phases, consistent with the recent observation that As associates with magnetite and other authogenic iron phases during iron reduction (28).

**Environmental Implications.** Arsenic elution in both abiotic and biotic columns indicates that As(III) is more mobile than As(V) under the flow conditions of this study. Additionally, reduction of Fe(III) suppressed As elution (i.e., enhanced retention), a result of enhanced sequestration during Fe(II)-induced transformation of ferrihydrite. Reductive dissolution of ferrihydrite, under the conditions of our study, did not contribute (and instead removed) As to the aqueous phase relative to abiotic systems.

The ratio of As to Fe (hydr)oxide present in contaminated soils and sediments is often low enough that near complete dissolution of Fe-bearing phases would be required to eliminate Fe-bearing minerals as sorbents of As. However, secondary Fe minerals formed during biotransformation could act as sorbents of As under reducing conditions. Thus, the capacity of many soil and aquifer minerals to sequester As through adsorption on or incorporation into secondary solid phases must be assessed in order to fully understand the partitioning of As between the aqueous and solid phase. Furthermore, and potentially most importantly, the relative binding strength (and extent of binding) of As(III) and As(V) to solids must be examined, particularly their rate of response to changes in dissolved concentrations (i.e., propensity for desorption). The kinetics of As(III) desorption from ferrihydrite, for example, appear to be more rapid than As(V) under dynamic flow at proportional surface coverage (relative to their respective adsorption maxima). If this is true for most subsurface minerals, As reduction may be the dominant mechanism controlling As mobilization under reducing conditions. Iron(II), often observed to increase with increased concentrations of As under anaerobic conditions, may indicate a corollary rather than causal relationship between iron (hydr)oxide reduction and As desorption. Transformation of Fe(III) minerals such as ferrihydrite can, in fact, decrease the extent of arsenic desorption rather than promote it.

## Acknowledgments

This work was supported by a U.S. EPA STAR graduate fellowship (EPA-FP916369) and the Stanford NSF Environmental Molecular Sciences Institute (NSF-CHE-0431425). We are grateful to Guangchao Li for analytical assistance and to Sam Webb for assistance with EXAFS fitting. Laboratory work and helpful commentary were provided by B. Stewart, Y. Masue, and T. Borch; constructive comments by 3 anonymous reviewers, and with input from the Associate Editor, further helped to improve this paper. We are indebted to John Bargar of the Stanford Synchrotron Radiation Laboratory and Matthew Newville of the Advanced Photon Source (GSECARS) for their assistance with XAS data collection and analysis. Portions of this work were performed at GeoSoilEnviroCARS (Sector 13), Advanced Photon Source (APS), Argonne National Laboratory. GeoSoilEnviroCARS is supported by the National Science Foundation - Earth Sciences (EAR-

0217473), Department of Energy - Geosciences (DE-FG02-94.ER14466), and the State of Illinois. Use of the APS was supported by the U.S. Department of Energy, Office of Science, Office of Basic Energy Sciences, under Contract No. W-31-109.-ENG-38. Portions of this research were also carried out at the Stanford Synchrotron Radiation Laboratory, a national user facility operated by Stanford University on behalf of the U.S. Department of Energy, Office of Basic Energy Sciences. The SSRL Structural Molecular Biology Program is supported by the Department of Energy, Office of Biological and Environmental Research, and by the National Institutes of Health, National Center for Research Resources, Biomedical Technology Program.

### Supporting Information Available

Metabolic activity within column experiments and lactate and acetate elution profiles (Figures S1 and S2) along with a comparison to total As and Fe eluted from As(V) loaded ferrihydrite-coated sand column (Figure S3) and linear combination fits of As-EXAFS spectra of column solids (Figure S4). This material is available free of charge via the Internet at <http://pubs.acs.org>.

### Literature Cited

- (1) Yu, W. H.; Harvey, C. M.; Harvey, C. F. Arsenic in groundwater in Bangladesh: A geostatistical and epidemiological framework for evaluating health effects and potential remedies. *Water Resour. Res.* **2003**, *39*, 1–17.
- (2) Smedley, P. L.; Kinniburgh, D. G. A review of the source, behaviour and distribution of arsenic in natural waters. *Appl. Geochem.* **2002**, *17*, 517–568.
- (3) McArthur, J. M.; Ravenscroft, P.; Safiulla, S.; Thirlwall, M. F. Arsenic in groundwater: Testing pollution mechanisms for sedimentary aquifers in Bangladesh. *Water Resour. Res.* **2001**, *37*, 109–117.
- (4) Ahmed, K. M.; Bhattacharya, P.; Hasan, M. A.; Akhter, S. H.; Alam, S. M. M.; Bhuyian, M. A. H.; Imam, M. B.; Khan, A. A.; Sracek, O. Arsenic enrichment in groundwater of the alluvial aquifers in Bangladesh: an overview. *Appl. Geochem.* **2004**, *19*, 181–200.
- (5) deLemos, J. L.; Bostick, B. C.; Renshaw, C. E.; Sturup, S.; Feng, X. H. Landfill-stimulated iron reduction and arsenic release at the Coakley Superfund Site (NH). *Environ. Sci. Technol.* **2006**, *40*, 67–73.
- (6) Dixit, S.; Hering, J. G. Comparison of arsenic(V) and arsenic(III) sorption onto iron oxide minerals: Implications for arsenic mobility. *Environ. Sci. Technol.* **2003**, *37*, 4182–4189.
- (7) Radu, T.; Subacz, J. L.; Phillippi, J. M.; Barnett, M. O. Effects of dissolved carbonate on arsenic adsorption and mobility. *Environ. Sci. Technol.* **2005**, *39*, 7875–7882.
- (8) Benner, S. G.; Hansel, C. M.; Wielinga, B. W.; Barber, T. M.; Fendorf, S. Reductive dissolution and biomineralization of iron hydroxide under dynamic flow conditions. *Environ. Sci. Technol.* **2002**, *36*, 1705–1711.
- (9) Hansel, C. M.; Benner, S. G.; Neiss, J.; Dohnalkova, A.; Kukkadapu, R. K.; Fendorf, S. Secondary mineralization pathways induced by dissimilatory iron reduction of ferrihydrite under advective flow. *Geochim. Cosmochim. Acta* **2003**, *67*, 2977–2992.
- (10) Gulens, J.; Champ, D. R.; Jackson, R. E. In *Chemical Modeling in Aqueous Systems*; Jenne, E. A., Ed.; American Chemical Society: Washington, DC, 1979; pp 81–95.
- (11) Zobrist, J.; Dowdle, P. R.; Davis, J. A.; Oremland, R. S. Mobilization of arsenite by dissimilatory reduction of adsorbed arsenate. *Environ. Sci. Technol.* **2000**, *34*, 4747–4753.
- (12) Oremland, R. S.; Stolz, J. F. The ecology of arsenic. *Science* **2003**, *300*, 939–944.
- (13) Silver, S.; Phung, L. T. Genes and enzymes involved in bacterial oxidation and reduction of inorganic arsenic. *Appl. Environ. Microbiol.* **2005**, *71*, 599–608.
- (14) Stolz, J. F.; Ellis, D. J.; Blum, J. S.; Ahmann, D.; Lovley, D. R.; Oremland, R. S. *Sulfurospirillum barnesii* sp nov and *Sulfurospirillum arsenophilum* sp nov., new members of the *Sulfurospirillum* clade of the epsilon Proteobacteria. *Int. J. Syst. Bacteriol.* **1999**, *49*, 1177–1180.
- (15) Fredrickson, J. K.; Zachara, J. M.; Kennedy, D. W.; Dong, H. L.; Onstott, T. C.; Hinman, N. W.; Li, S. M. Biogenic iron mineralization accompanying the dissimilatory reduction of hydrous ferric oxide by groundwater bacterium. *Geochim. Cosmochim. Acta* **1998**, *62*, 3239–3257.
- (16) Saltikov, C. Department of Environmental Toxicology, University of California–Santa Cruz, personal communication, 2005.
- (17) Herbel, M. J.; Blum, J. S.; Hoef, S. E.; Cohen, S. M.; Arnold, L. L.; Lisak, J.; Stolz, J. F.; Oremland, R. S. Dissimilatory arsenate reductase activity and arsenate-respiring bacteria in bovine rumen fluid, hamster feces, and the termite hindgut. *FEMS Microbiol. Ecol.* **2002**, *41*, 59–67.
- (18) Schwertmann, U.; Cornell, R. M. *Iron Oxides in the Laboratory: Preparation and Characterization*; Weinham: New York, 1991.
- (19) Herbel, M. J.; Fendorf, S. Biogeochemical processes controlling the speciation and transport of arsenic within iron coated sands. *Chem. Geol.* **2006**, *228*, 16–32.
- (20) Manning, B. A.; Martens, D. A. Speciation of arsenic(III) and arsenic(V) in sediment extracts by high-performance liquid chromatography hydride generation atomic absorption spectrophotometry. *Environ. Sci. Technol.* **1997**, *31*, 171–177.
- (21) Stookey, L. L. Ferrozine - a new spectrophotometric reagent for iron. *Anal. Chem.* **1970**, *42*, 779–8.
- (22) Webb, S. *Sixpack v.0.53*; Stanford Synchrotron Radiation Laboratory: Menlo Park, CA, U.S.A., 2005.
- (23) Thorat, S.; Rose, J.; Garnier, J. M.; Van Geen, A.; Refait, P.; Traverse, A.; Fonda, E.; Nahon, D.; Bottero, J. Y. XAS study of iron and arsenic speciation during Fe(II) oxidation in the presence of As(III). *Environ. Sci. Technol.* **2005**, *39*, 9478–9485.
- (24) Zachara, J. M.; Kukkadapu, R. K.; Fredrickson, J. K.; Gorby, Y. A.; Smith, S. C. Biomineralization of poorly crystalline Fe(III) oxides by dissimilatory metal reducing bacteria (DMRB). *Geomicrobiol. J.* **2002**, *19*, 179–207.
- (25) Appelo, C. A. J.; Van der Weiden, M. J. J.; Tournassat, C.; Charlet, L. Surface complexation of ferrous iron and carbonate on ferrihydrite and the mobilization of arsenic. *Environ. Sci. Technol.* **2002**, *36*, 3096–3103.
- (26) Thanabalasingam, P.; Pickering, W. F. Arsenic sorption by humic acids. *Environ. Pollut. B* **1986**, *12*, 233–246.
- (27) Lin, H. T.; Wang, M. C.; Li, G. C. Complexation of arsenate with humic substance in water extract of compost. *Chemosphere* **2004**, *56*, 1105–1112.
- (28) Islam, F. S.; Pederick, R. L.; Gault, A. G.; Adams, L. K.; Polya, D. A.; Charnock, J. M.; Lloyd, J. R. Interactions between the Fe(III)-reducing bacterium *Geobacter sulfurreducens* and arsenate, and capture of the metalloid by biogenic Fe(II). *Appl. Environ. Microbiol.* **2005**, *71*, 8642–8648.

Received for review June 29, 2006. Revised manuscript received September 3, 2006. Accepted September 5, 2006.

ES061540K